Journal of Industrial Microbiology & Biotechnology (2019) 46:809–818
https://doi.org/10.1007/s10295-019-02152-y

METABOLIC ENGINEERING AND SYNTHETIC BIOLOGY - ORIGINAL PAPER

Lipidomics characterization of the alterations of *Trichoderma brevicompactum* membrane glycerophospholipids during the fermentation phase

Yunfan Bai[1] · Yuran Gao[1] · Xin Lu[1] · Huiyu Wang[2]

Received: 12 November 2018 / Accepted: 12 February 2019 / Published online: 7 March 2019

Abstract
The biological membrane lipid composition has been demonstrated to greatly influence the secretion of secondary metabolites. This study was conducted to investigate the periodical alterations of whole cellular lipids and their associations with secondary products in *Trichoderma brevicompactum*. An electrospray ionization–mass spectrometry-based lipidomics strategy was used to acquire the metabolic profiles of membrane lipids during fermentation. Univariate analyses showed that most fungi glycerophospholipids were significantly altered at the early phase compared with the late phase. In addition, correlation analyses showed high correlations between phosphatidylcholine alterations and fermentation duration. In addition, the fermentation-associated alterations of phosphatidylcholines were found to be in accordance with the degrees of unsaturation of acyl-chains. Harzianum A reached a maximum on the 12th day, while trichodermin and 6-pentyl-2*H*-pyran-2-one showed the highest abundances on the 9th day, both of which were inclined to correlate with the alterations of phosphatidylcholines and phosphatidylethanolamines, respectively. These findings demonstrated that the alterations of the membrane lipid species in *Trichoderma* spp. were associated with the fermentation phases and might influence the secretion of specific secondary products, which may be useful in studying the optimization of secondary products in *Trichoderma* spp.

Keywords *Trichoderma brevicompactum* · Metabolic profile · Lipidomics · Secondary product · Glycerophospholipid

Introduction

Trichoderma spp. are a category of free-living fungi that are widely found in root, soil and foliar environments [31]. They are known by their applicable characteristics, including excreting antibiotic substances, competing with other microorganisms for ecological niches, producing enzymes to degrade fungi cell walls, and so on [3, 12, 20, 21]. As reported, the use of small molecules secreted by *T. brevicompactum*, such as trichodermin, gliotoxin, small peptides, volatile pyropes and lactones, is a primary mechanism for biocontrol in forest protection [22, 35, 36]. Several studies have demonstrated the correlation between the secretion of small molecules and the membrane fluidity of fungi, the latter of which is strongly associated with the biochemical compositions of the membrane lipids [17, 34]. Thus, the characterization of the periodic alterations of the membrane lipids in fungi is of great significance to maximize product yields for biocontrol.

Lipidomics, a new branch of metabolomics, refers to the qualitative and quantitative determinations of stimuli-dependent changes of the lipid species in organisms [10, 24, 33]. As one of the primary membrane lipids, glycerophospholipid (GPL) plays a critical role in cell signaling and the change of material during various biological events [11, 19]. For instance, phosphatidylethanolamines (PEs) are known for their participation in membrane fusion and fission steps during endocytosis, exocytosis, cytokinesis, and vesicle trafficking. Phosphatidylserines (PSs) and phosphatidylinositols (PIs) have been shown to continuously interact with many regulatory factors during cellular signaling transduction [13,

Electronic supplementary material The online version of this article (https://doi.org/10.1007/s10295-019-02152-y) contains supplementary material, which is available to authorized users.

✉ Huiyu Wang
wanghuiyuwhy@163.com

[1] School of Life Science and Technology, Harbin Institute of Technology, Harbin City, China

[2] School of Pharmacy, Qiqihar Medical University, No. 333, North Bukui Street, Qiqihar City 161000, China

30]. Xia et al. found that alterations in lipid compositions tended to disturb membrane fluidity, resulting in changes in the fermentative productivity of *Saccharomyces cerevisiae* 424A (LNH-ST) and its parental strain 4124 [34]. Similarly, the yields and classes of secondary metabolites in *Trichoderma* spp. were also found to vary during the fermentative cycle, which would undoubtedly influence the production of applicable secondary metabolites [2, 23]. Nevertheless, knowledge relevant to the association between the periodical changes of products in *Trichoderma* spp. and the compositions of membrane lipids is still lacking.

In the present study, to investigate the alterations of the whole cellular lipids associated with fermentative periods and secondary products, the primary membrane lipids involving PCs, PEs and PSs in sequential growth phases in *T. brevicompactum* were characterized using an electrospray ionization–mass spectrometry (ESI–MS)-based lipidomics strategy. Meanwhile, fermentation media were also characterized with ultra-performance liquid chromatography coupled to mass spectrometry (UPLC-MS) to observe the changes of secondary metabolites due to fermentative periods. Principle component analysis (PCA) was conducted to observe the global alterations of GPLs during growth. Student's *t* test was applied to characterize the differential significance of lipids between the early and late phases. The double bond equivalent versus carbon number plot (DVC) was also constructed to characterize the alteration patterns regarding to the diversity of the lipid structures. Correlation network analysis was conducted to reveal the relationships between the primary products and the altered lipid species. In summary, this study hopefully provides helpful references for optimizing biocontrol strategies and helps to clarify the relationship between lipid compositions and the secretion of secondary products.

Materials and methods

Reagents and chemicals

Potatoes were obtained from local retail stores in Harbin, China. Dextrose and agar were purchased from Sanland (Los Angeles, CA, USA). Methanol and acetonitrile (HPLC grade) were provided by Fisher Scientific (Waltham, MA, USA). Isopropanol, ammonia water, and formic acid (HPLC grade) were purchased from Fluka (St. Louis, MO, USA). Deionized water was produced by a Milli-Q ultrapure water system (Millipore, Billerica, USA). Methyl tert-butyl ether (HPLC grade) was provided by Aladdin (Shanghai, China).

Culture media and fungal strain

Potato dextrose agar (PDA) medium (g/L)

Potato, 200 g; dextrose, 20.0 g; agar, 20.0 g; distilled water, 1000 mL, adjusted to pH 6.0 before autoclaving (at 121 °C for 20 min).

Potato dextrose (PD) medium (g/L)

Potato, 200 g; dextrose, 20.0 g; distilled water, 1000 mL, adjusted to pH 6.0 before autoclaving (at 121 °C for 20 min).

Fungal strain

The fungal strain *T. brevicompactum* strain separated from soil was sponsored by the Forest Department at the Northeast Forest University (Harbin, China), and identified using 16S rDNA sequence and morphology analysis. The selected fungi were stored on PDA slants at 4 °C for further use.

T. brevicompactum culture

Fresh mycelia were picked and inoculated on PDA plates in the dark for 4 days at 28 °C. Then, three young mycelial pieces (6-mm diameter) grown on PDA were cut from the margins of the colony and placed into 350-mL flasks containing 100 mL PD medium. The pieces were further cultured at 28 °C in a rotary shaker at 150 rpm. The negative control was prepared by mixing three PDA pieces (6-mm diameter) with 100 mL PD medium under the same conditions. For the cultivation time, the fungal biomass was periodically harvested from the 3rd day to the 15th day in 3-day intervals. Each harvesting group had three replicates.

Sample preparation

Trichoderma brevicompactum mycelia and fermentation media were separated via centrifugation at 4 °C, 12,000*g* for 15 min and the mycelia were further dried via freeze-drying. For the extraction of whole cellular lipid species, 5 mg of dried mycelia were added by 450 μL of 75% methanol and cracked by sonication at 30 Hz for 2 min in ice-water bath. After being centrifuged at 12,000*g* for 15 min, 400 μL of the supernatant was isolated and added by 1000 μL of methyl tert-butyl ether (MTBE), followed by incubation in oscillator at 1000 rpm for 10 min. Then, the mixture was added by 250 μL of deionized water and mixed by vortexing for 1 min. After being centrifuged at 12,000*g* for 15 min, 800 μL of the upper layer supernatant was isolated from the mixture and dried by rotating vacuum. Fermentation media were filtered

by a 0.45-μm disposable polytetrafluoroethylene (PTFE) filter, and 2 mL of the filtered media were dried by freeze-drying. At last, both dried residues were stored at − 80 °C until analysis.

ESI–MS analysis

The dried fermentation media harvested at the start of the fermentation (as the background) and the dried mycelia residuals were dissolved in chloroform:methanol 1:2 (v:v) for direct infusion injection. Prior to analysis, formic acid was added by 0.1% (v/v), and the solution was injected into a Quattro Micro triple quadrupole mass spectrometer (Micromass, Manchester, UK) equipped with a dual electrospray ionization (ESI) source at a flow rate of 10 μL/min. PCs, PEs and PSs were analyzed in positive mode at collision energy values ranging from 25 to 30 eV in the precursor ion scan mode based on specific fragments of the corresponding lipid species. Argon was used as the collision gas. The (Lyso)PCs were acquired by the product ion of *m/z* 184, while PEs and PSs were acquired by neutral losses of 141 and 87, respectively. The mass spectra were processed by MassLynx software (Waters, Milford, USA). The lipid species were abbreviated as follows: lipid abbreviation (total carbon number in the chains: total number of double bonds in the chains).

UPLC-MS analysis

The dried fermentation media of cultivation times were redissolved in 100 μL of acetonitrile and 5 μL of the supernatant and were injected after centrifugation.

The chromatographic separation was performed using an ultra-performance liquid chromatography (UPLC) system (Waters, Milford, USA) equipped with a column of BEH C_{18} 2.1 mm × 100 mm, 1.7 μm (Waters, Milford, USA). The mobile phase A was acetonitrile containing 0.1% formic acid, and the mobile phase B was deionized water containing 0.1% formic acid for the positive ion mode, while 0.1% ammonium hydroxide was added into both phases for the negative ion mode.

For chromatographic separation, a linear gradient was run at a flow rate of 300 μL/min and compiled as follows: 1% A was held from the initial start to 0.5 min; 1-15% A was held from 0.5 to 4.0 min; 15–55% A was held from 4.0 to 4.5 min; 55–90% A was held from 4.5 to 11.5 min; 90–99% A was held from 11.5 to 12.0 min followed by an isocratic elution at 99% A for 3 min; and the gradient was then changed back to 1% A from 15.0 to 15.1 min, followed by an equilibration for 1 min. During the analyses, the column temperature was set at 40 °C.

Statistical analysis

Student's *t* tests were performed to characterize the differential significances of lipids between the groups. The correlation coefficients were measured with Spearman correlation analysis. Both PCA and PLS-DA were constructed to reveal the global clustering layouts of GPLs between the different fermentation phases. Double bond equivalence (DBE) versus carbon number plot was built upon the lipids of each individual species to explore the changing patterns associated with the chain length and degree of unsaturation (DOU). Based on a logistic model, the growth curve over the 15 days was established to explore the growth pattern of *T. brevicompactum.* The correlation network was constructed by cytoscape v.3.5.1. PCA and PLS-DA were performed with Ezinfo 2.0. DVC plots were realized using Origin 8.0. Other computational and statistical methods were conducted with R platform v.2.14.2.22.

Results

Lipidomics profiling analysis

Based on the shotgun lipidomics strategy, 128 lipid species including 5 LysoPCs, 7 LysoPEs, 11 LysoPSs, 41 PCs, 30 PEs, and 34 PSs were identified (Table S1), and nearly, no lipid species were detected in the dried fermentation media at the start of the fermentation, indicating no exogenous lipids existed in the culture environment.

To globally evaluate the metabolic alterations of GPLs of whole cellular during the different growth phases of *T. brevicompactum*, both PCA and PLS-DA models were constructed based on 128 GPLs. As shown in the PCA score plot (Supplementary Fig. S1), no obvious outliers could be observed, demonstrating the robustness of the dataset. In the PLS-DA score plot (Fig. 1a), the clustering pattern showed that samples at the same fermentation times were located together, whereas samples from different phases were separated from each other. The grouping trend was arranged orderly along with the extension of fermented days. In detail, the samples of the early phase were located on the left side of the first principal component (PC1), the samples of the middle phase were near the geometry, and the samples of the late phase were scattered on the right. The corresponding validation plot (Supplementary Fig. S2) illustrated that no overfitting emerged in the PLS-DA model. Notably, the trend from the 3rd day to the 6th day was opposite to the overall trend, demonstrating the unsteady metabolism during the early phases.

The loading biplot mainly showed the grouping contributions of different types of GPLs to the grouping layout. As shown in Fig. 1b, d, LysoPCs and PCs mainly gathered on

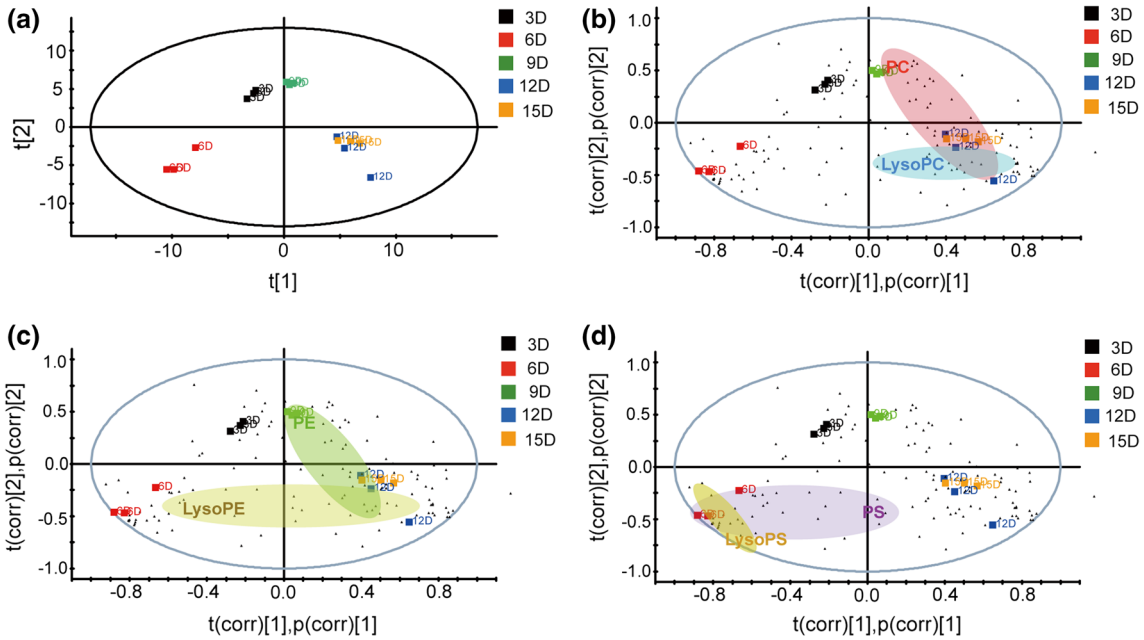

Fig. 1 Score plot and loading bi plots of PLS-DA model constructed with 128 lipid species in *T. brevicompactum* mycelia. **a** Score plot; **b** loading bi plot with LysoPCs and PCs indicated; **c** loading bi plot with LysoPEs and PEs indicated; **d** loading bi plot with LysoPSs and PSs indicated. Black, red, green, blue, yellow boxes indicate the *T. brevicompactum* mycelia collected on the 3rd day, the 6th day, the 9th day, the 12th day, and the 15th day, respectively during fermentation. Black triangles represent lipid species (color figure online)

the right side of PC1, while LysoPSs and PSs scattered at the bottom, demonstrating that GPLs of different categories exhibited different alteration patterns as the fermentation proceeded. LysoPCs were mainly excreted on the 12th day, while PCs were excreted on the 9th day, the 12th day and the 15th day. PSs and LysoPSs were mostly secreted on the 6th day. Comparably, PEs and LysoPEs distributed more widely along with PC1 (Fig. 1c). PCs and LysoPCs were positively correlated with PC1, while PSs and LysoPSs were generally negatively correlated with PC1. Therefore, it could be deduced that (Lyso)PCs, (Lyso)PSs, and (Lyso)PEs generally revealed increased, decreased and call-back tendencies, respectively, during fermentation.

Differential significances of GPL species during the fermentation growth phases

Student's *t* test and Spearman correlation analysis were conducted on each GPL species and category for the characterizations of differential tendencies and significances of GPLs in *T. brevicompactum* along fermentation.

The 6th day and the 15th day were chosen to present the early and late growth phases, because they were scattered at the left and right ends of the PCA score plot, respectively. As shown in Fig. 2a, majority of PCs, PEs, and PSs revealed significant changes ($p < 0.05$) between the 6th day and the 15th day.

To further evaluate the correlations between the alterations in the GPLs and the sequential fermentation periods, Spearman correlation analysis was carried out based on each GPL at the different fermentation periods. As presented in Fig. 2b, PCs showed high correlations with days of fermentation (average correlation coefficient = 0.655), while the average correlation coefficients of PEs and PSs were 0.447 and 0.432, respectively. The above results were generally consistent with the performances that PCs, PEs, and PSs revealed in the loading biplot, indicating that the alterations of the majority of the GPLs were correlated with fermentation duration.

DVC analysis

To more specifically characterize the alteration diversity associated with the acyl-chain structures of the lipids in each category, carbon numbers (CNs) and DBEs in the acyl-chains of each lipid were summarized to construct the DVC plots, in which the fold-change (FC) values between the 6th day and the 15th day of GPLs were imported for visualization.

As shown in Fig. 3, the FC values of PCs with the same CNs exhibited significant DBE associated alterations. Specifically, in the PCs with CNs of 34 and 40, the FC values increased as the DBEs increased (from 0 to 4). For the PCs with a CN of 36, FC values showed a clear call-back tendency as DBE increased that the FCs increased from DBE

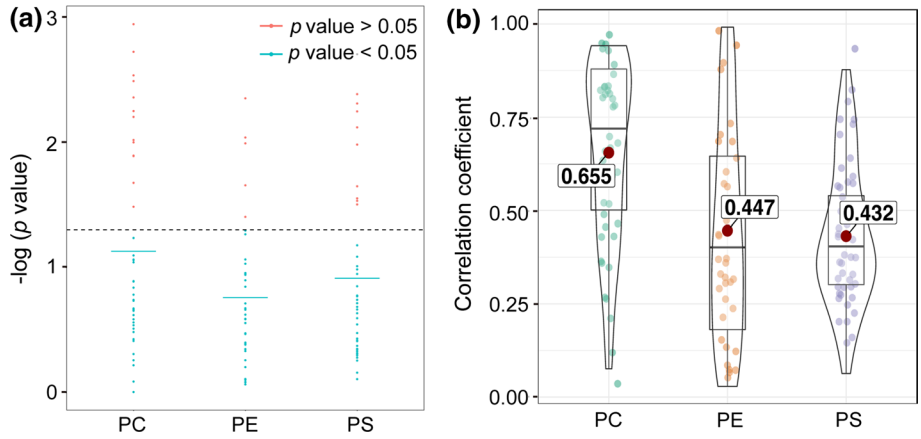

Fig. 2 Univariate analysis of 128 lipid species in different lipid categories (PC, PE, PS) between the 6th day and the 15th day of *T. brevicompactum* mycelia. **a** –Log(*p*) values of Student's *t* tests, red dots are the lipid species showing *p* values larger than 0.05, blue dots are the lipid species showing *p* values smaller than 0.05, blue solid lines indicate the means of the *p* values in each lipid category; **b** Spearman correlation analyses of different lipid categories (PC, PE, PS) with growth phases. Blue, orange, and purple dots indicate PC, PE, PS lipid species, respectively. Red dots indicate the means of correlation coefficients (color figure online)

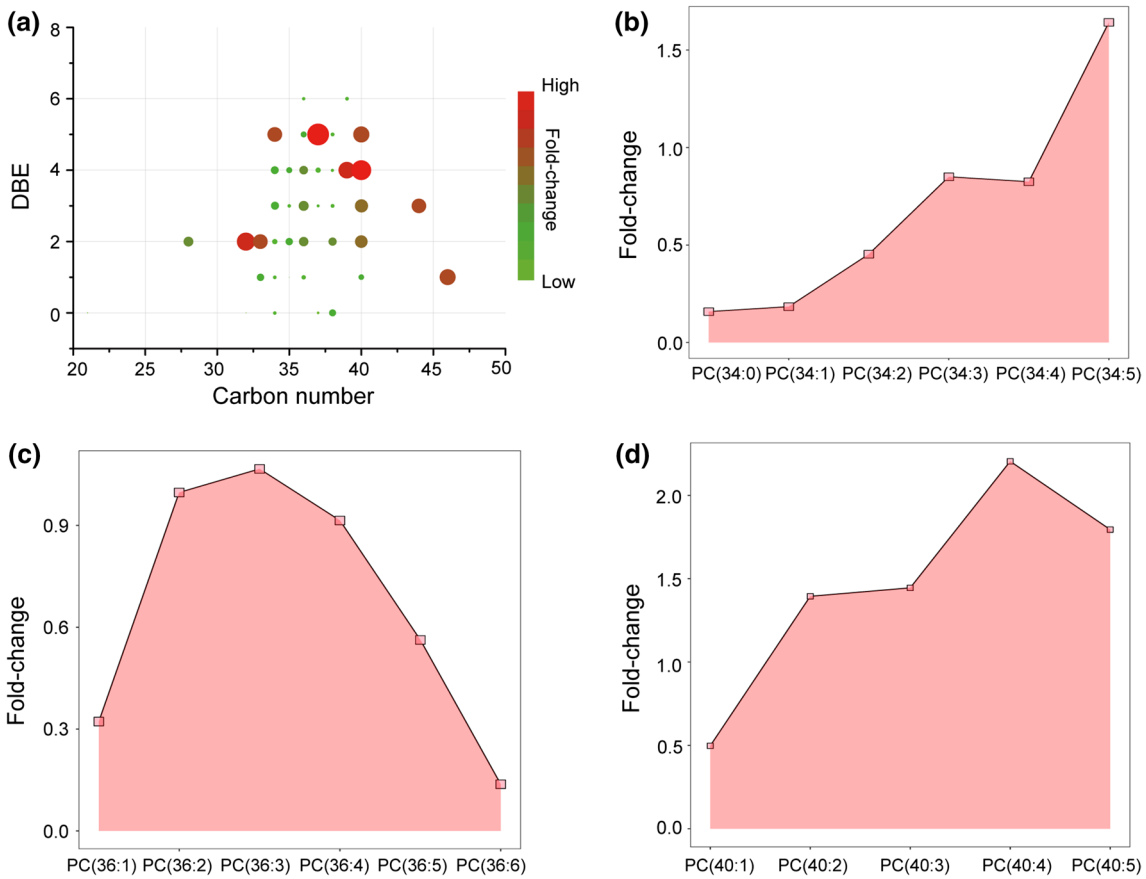

Fig. 3 Acyl chain-associated alterations of PCs on the 15th day compared to the 6th day **a** Double bond equivalence versus carbon number plot of PCs. Colors and sizes of dots indicate different degrees of fold-change; **b** fold-change values of PCs with CN of 34; **c** fold-change values of PCs with CN of 36; **d** fold-change values of PCs with CN of 40 (color figure online)

values of 1–3 and decreased from DBE values of 3–6. These findings demonstrated that the alterations of the FCs in PCs varied in accordance with the structural diversity of the acyl-chains. However, no clear fermentation duration-associated manners were observed in the DVCs of PEs, PSs, and other CNs of PCs. (Supplementary Fig. S3).

Secondary products in the fermentation media

A total of three metabolites were identified in the fermentation media, i.e., harzianum A, trichodermin, and 6-pentyl-2*H*-pyran-2-one, which have been proven to play active roles in the application of *Trichoderma* spp. for biocontrol.

As shown in Fig. 4a–c, the secretion of the three secondary metabolites exhibited similar pattern along with fermentation phase, in which all three metabolites presented increased and decreased tendencies during fermentation, respectively. Harzianum A reached its maximum on the 12th day, while 6-pentyl-2*H*-pyran-2-one and trichodermin reached their peak values on the 9th day, and all metabolites showed gradual decreases in the following phases. The growth curve based on the logistic model (Fig. 4d) revealed an overall growth process. The first phase is the lag phase, in which no changes in dry weight were measured and the growth rate was relatively low. The second phase was the log phase, in which a rapid increase in the biomass dry weight was observed and the growth curve reached its maximal slope. The third phase was the deceleration phase, in which the slope of the growth curve continuously decreased. The last phase was the stationary phase, where there were no changes in the biomass dry weight [7].

Network analysis and correlation analysis

To further investigate the influences of lipid compositions on the release of the secondary products, Spearman correlation analyses were conducted between the lipid species and the excreted products. Correlation networks were further constructed based on the criteria of the absolute values of the correlation coefficients being larger than 0.8. Consequently, three LPCs, seventeen PCs, three LPEs, three PEs, and three PSs were highly correlated with harzianum A in the network diagram. In addition, trichodermin and 6-pentyl-2*H*-pyran-2-one were connected with each other, and meanwhile, four PEs, two PCs, one LPE, three PSs were linked with trichodermin, while seven PEs, three PCs, one PS, and one LPS were associated with 6-pentyl-2*H*-pyran-2-one (Fig. 5a). We also found most PCs were correlated with harzianum A (average correlation coefficients = 0.645), and most PEs were inclined to be correlated with trichodermin (average correlation coefficients = 0.521), suggesting the potential relationship of the secretion of these compounds with the GPLs components (Supplementary Fig. S4).

The correlation coefficients between the secondary metabolite secretion and growth phases were also calculated to explore the component pattern over time (Supplementary Fig. S5b). Harzianum A was highly associated with the growth phase (average correlation coefficients = 0.890),

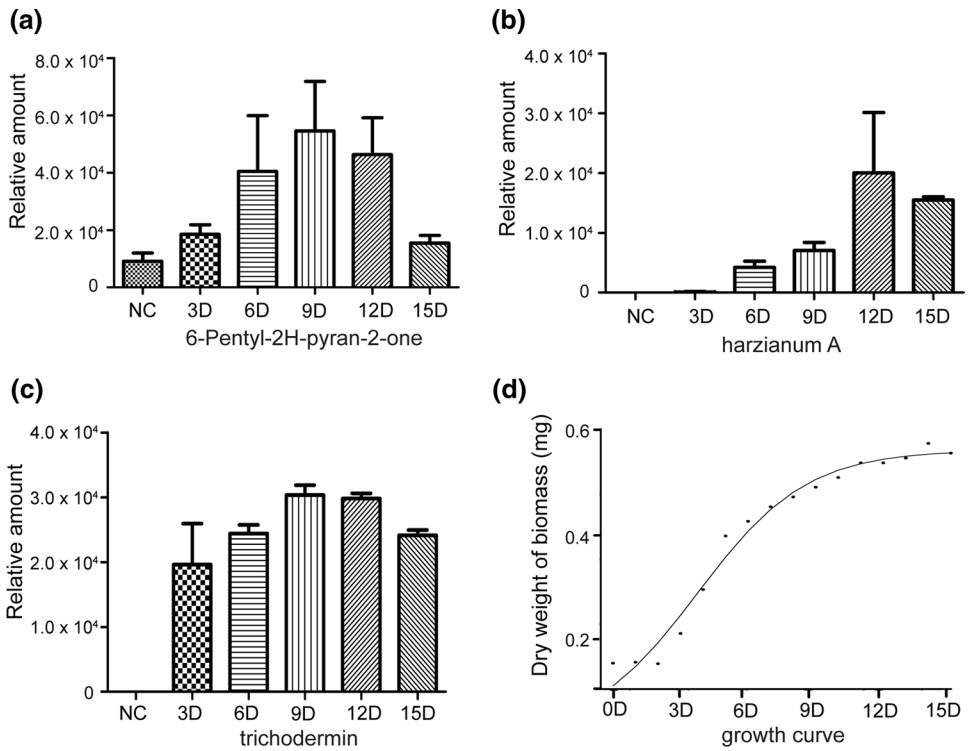

Fig. 4 Alterations of secondary metabolites in the media of different fermentation phases. **a** 6-Pentyl-2*H*-pyran-2-one; **b** harzianum A; **c** trichodermin and **d** growth curve for *T. brevicompactum* for 15 days based on a logistic model

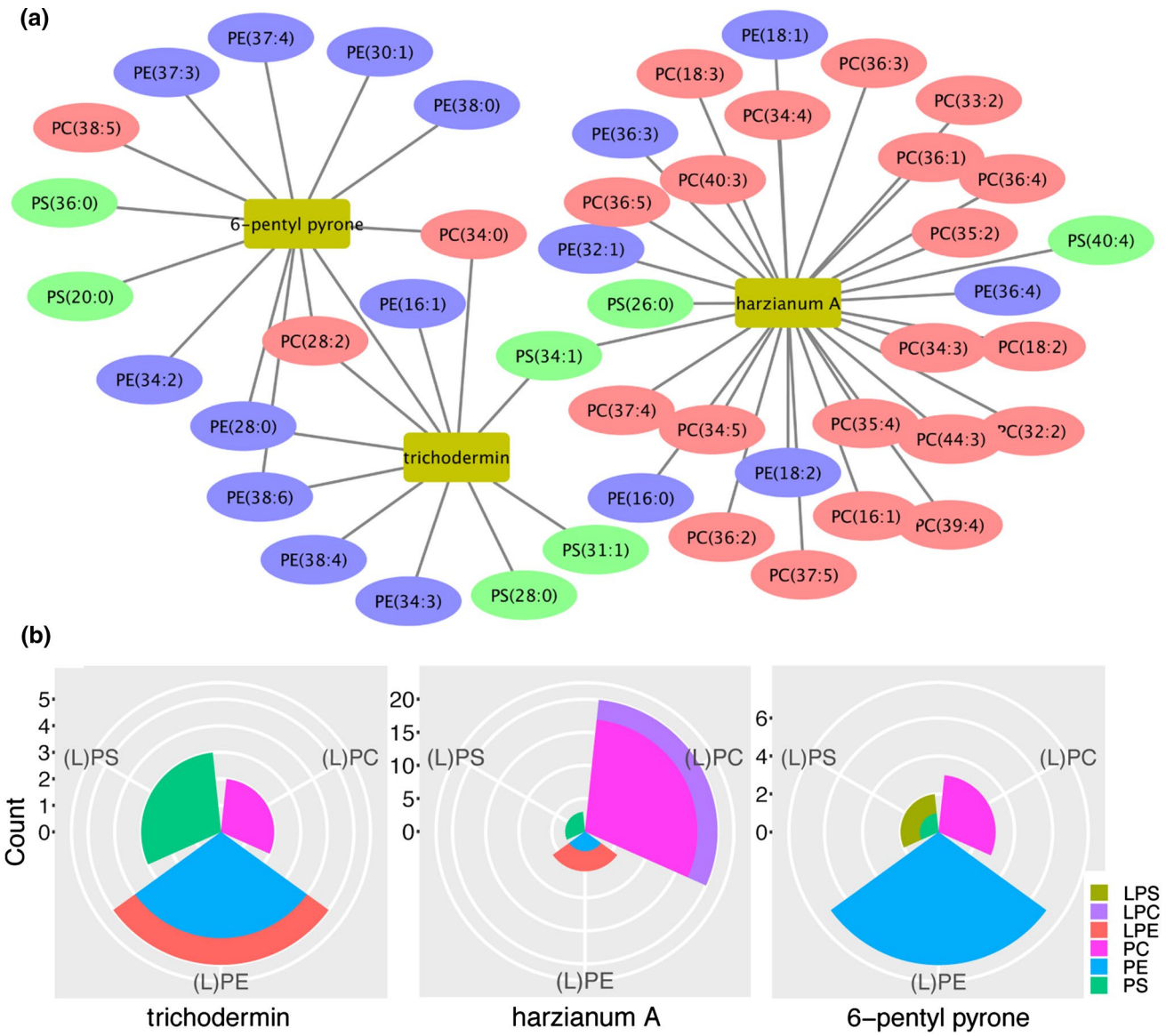

Fig. 5 Correlation network and Spearman correlation coefficients of secondary metabolites with different types of lipids. **a** Correlation network constructed with lipid species and secondary metabolites (Correlation coefficient > 0.8). Red, blue and green nodes represent PCs, PEs, and PSs, respectively. Yellow boxes indicate the secondary metabolites. **b** Numbers of lipid species with correlation coefficients > 0.8. Pea green, purple, red, pink, blue, green represent LPSs, LPCs, LPEs, PCs, PEs, and PSs, respectively (color figure online)

while there was no such manner observed with the other two metabolites.

Discussion

Trichoderma spp., as biological control agents, have proven to be capable of secreting a spectrum of active biochemicals [3]. However, only a small number of *Trichoderma* spp. have been studied for their biocontrol activities. As thus, the metabolite secretion pattern and biocontrol mechanisms need to be fully understood, as both play important roles in improving biocontrol capabilities. This present study initially demonstrated that the GPL profiles were significantly altered in *Trichoderma brevicompactum* during the fermentation periods and presented the close association between the membrane lipid compositions and the three key biocontrol-related metabolites (harzianum A, trichodermin, and 6-pentyl-2*H*-pyran-2-one).

GPLs, mainly PCs, PEs and PSs, have varied structures with different polar heads at the sn-3 position of the glycerol backbone. Among them, PCs and PEs are the most abundant GPLs in the biological membranes. PCs normally act as the bilayer-stabilizing lipids for membrane construction, and

PEs also have a strong propensity to form nonbilayer hexagonal phases [19]. Therefore, PCs and PEs play crucial roles in maintaining membrane integrity and cellular functions [32]. As another important GPL, PSs are mainly produced by the transformation with PEs and PCs via the exchanges of head groups [19]. These GPL species have been demonstrated to greatly influence the cellular functionalities of organisms, including mammalian cells and fungi. Xia et al. found that PSs were closely related to the fungi growth rate, and PCs, PEs were also capable of affecting the glucose utilization rates in the yeast strain *Saccharomyces cerevisiae* 424A (LNH-ST) and its parental strain 4124 [34]. Bernat et al. found that ROS generation in the filamentous fungi *Cunninghamella elegans* treated with tributyltin might be correlated with the variation of lipid profiles [4]. Gao et al. demonstrated that cellular phospholipid homeostasis had the ability to regulate fungal growth, cell polarity, differentiation, and virulence [11]. In addition, the production of phospholipid molecular classes was found to be phase-dependent [18]. In this study, different lipid metabolic patterns proved to be correlated with fermentation periods, while three important biocontrol metabolites varied in accordance with the alterations of the GPLs. These results may reveal that lipid compositions have significant impacts on metabolite secretion and may further reflect fungi functionalities.

The chain length and degree of unsaturation of acyl-chain are the basic characteristics of lipids and play key roles in the determination of many cellular functions, such as cell protection, recognition, and material transition [25, 26]. Yan et al. compared the DBE features of the membrane lipid species in three different strains to explore the ecophysiological diversity among them [37]. Kabelitz et al. demonstrated that the changes in the degree of saturation of membrane lipids associated with the membrane fluidity of *Acinetobacter calcoaceticus* after stimulation by aliphatic alcohols [16]. In this study, PCs with specific CNs revealed altering patterns with the increases of DBE values that might be associated with the alterations in membrane fluidity.

Among the volatile antifungal compounds produced by the *Trichoderma* strains, the most well-documented is 6-pentyl pyrone, a polyketide with a sweet coconut-like aroma [27]. 6-pentyl pyrone and its derivates have been known for inhibiting the growth of several plant–pathogenic fungi, such as *Armillaria mellea* (Tarus et al. [27]) [15]. Similarly, 6-*n*-pentyl-2*H*-pyran-2-one was reported to block the production of deoxynivalenol by *Fusarium graminearum* (Cooney et al. [8]) [8]. Trichodermin is another promising inhibitor of protein synthesis via the blockage of the peptidyltransferase center of the 60-S subunit of the 80-S type ribosomes, resulting in the antifungal activity against many phytopathogenic fungi, such as *B. cinerea* [6, 28, 35, 38]. Xu et al. investigated the inhibitory activity of trichodermin against the mycelial growth of plant–pathogenic fungi that suggested its potential in agricultural applications [36]. Harzianum A is structurally similar to trichoverroid, which is mainly isolated from *T. harzianum* fermentation, and shows the strongest activity in the inhibition of fungi *C. albicans* and *S. cerevisiae* [9]. The primary bottleneck in the application of secondary metabolites for biocontrol is the low yield during fermentation. Therefore, the optimization of the fermentation factors, especially the harvesting time, is of great applicable significance for the production of secondary metabolites in biocontrol. In the present study, harzianum A reached the highest yield on the 9th day, while trichodermin and 6-*n*-pentyl-2*H*-pyran-2-one reached the highest concentrations on the 12th day. Notably, the fermentation phase from the 9th day to the 12th day was the deceleration phase in the growth curve of *T. brevicompactum*, which was typically considered the right time to extract secondary metabolites. In addition, the secretion of these compounds was also correlated with the alterations of GPLs during fermentation. For the knowledge regarding to the association between membrane lipid components and secondary metabolite production, GPLs have been proven to play active roles in the secretion of metabolites [17]. A potential explanation for this manner is that the fermentative metabolic enzymes are often compartmentalized to specific organelles, membrane lipids of which periodically alter during fermentation, resulting in the correlated alterations of the metabolites in amount and category [34]. Besides, compositions and spatial distributions of lipid species can also modulate membrane biophysical properties including fluidity, flexibility, and thickness, which may affect the secretion of small molecules during specific biological events [5, 14, 29]. In addition to the GPLs presented in this study, there are many other lipids such as sterol and fatty acids have been proven to be associated with membrane fluidity [1]. Therefore, studies focusing on subcellular organelle lipidomics and other kinds of lipids would be of great significance in understanding the correlation between lipid alteration and the cell fermentative capacity.

Conclusion

In the present study, an ESI–MS-based lipidomics strategy was conducted to explore the metabolic alterations of GPLs in *Trichoderma brevicompactum* during fermentation. Majority of the GPLs including PCs, PEs, and PSs were correlated with fermentation duration, and presented significant alterations between early and late growth phase. Structural diversity of the acyl-chains was associated with the alterations in some kinds of GPL species. Three main biocontrol-related metabolites were detected in the media and their secretion patterns during fermentation were correlated with specific GPLs. This study may provide researchers with the reference for optimizing biocontrol strategies and helps

to clarify the relationship between lipid compositions and the secretion of secondary products.

Acknowledgements This study was funded by the Science and Technology Project of Qiqihar City (SFGG-201543) and the Doctoral Scientific Fund Project (QY2015B-03). We sincerely express our appreciation to the Forest Department in Northeast Forest University for donating the *Trichoderma brevicompactum* strain to this study.

Compliance with ethical standards

Conflict of interest The authors declare that they have no conflict of interest.

References

1. Alexandre H, Rousseaux I, Charpentier C (1994) Relationship between ethanol tolerance, lipid composition and plasma membrane fluidity in *Saccharomyces cerevisiae* and *Kloeckera apiculata*. FEMS Microbiol Immunol 124:17–22. https://doi.org/10.1111/j.1574-6968.1994.tb07255.x
2. Bailey MJ, Tahtiharju J (2003) Efficient cellulase production by *Trichoderma reesei* in continuous cultivation on lactose medium with a computer-controlled feeding strategy. Appl Microbiol Biotechnol 62:156–162. https://doi.org/10.1007/s00253-003-1276-9
3. Benítez T, Rincón AM, Limón MC et al (2005) Biocontrol mechanism of *Trichoderma* strains. Int Microbiol 7(4):249–260
4. Bernat P, Gajewska E, Szewczyk R et al (2014) Tributyltin (TBT) induces oxidative stress and modifies lipid profile in the filamentous fungus *Cunninghamella elegans*. Environ Sci Pollut Res Int 21:4228–4235. https://doi.org/10.1007/s11356-013-2375-5
5. Boeszebattaglia K, Schimmel R (1997) Cell membrane lipid composition and distribution: implications for cell function and lessons learned from photoreceptors and platelets. J Exp Biol 200(Pt 23):2927. https://doi.org/10.1016/s0006-3495(02)75223-5
6. Carrasco L, Barbacid M, Vazquez D (1973) The trichodermin group of antibiotics, inhibitors of peptide bond formation by eukaryotic ribosomes. Bba 312(2):368–376. https://doi.org/10.1016/0005-2787(73)90381-x
7. Classen JJ, Engler CR, Kenerley CM, Whittaker AD (2000) A logistic model of subsurface fungal growth with application to bioremediation. J Environ Sci Health A Tox Hazard Subst Environ Eng 35:465–488. https://doi.org/10.1080/10934520009376982
8. Cooney JM, Lauren DR et al (1997) Effect of solid substrate, liquid supplement, and harvest time on 6-*n*-Pentyl-2*H*-pyran-2-one (6PAP) Production by *Trichoderma* spp. J Agric Food Chem 45(2):531–534. https://doi.org/10.1021/jf960473i
9. Corley DG, Millerwideman M, Durley RC (1994) Isolation and structure of harzianum A: a new trichothecene from trichoderma harzianum. J Nat Prod 57(3):422–425. https://doi.org/10.1021/np50105a019
10. Dennis EA (2009) Lipidomics joins the omics evolution. Proc Natl Acad Sci U S A 106(7):2089–2090. https://doi.org/10.1073/pnas.0812636106
11. Gao Q, Lu Y, Yao H et al (2016) Phospholipid homeostasis maintains cell polarity, development and virulence in metarhizium robertsii. Environ Microbiol 18:3976–3990. https://doi.org/10.1111/1462-2920.13408
12. Harman GE, Howell CR, Viterbo A et al (2004) Trichoderma species–opportunistic, avirulent plant symbionts. Nat Rev Microbiol 2:43–56. https://doi.org/10.1038/nrmicro797
13. Hishikawa D, Hashidate T, Shimizu T et al (2014) Diversity and function of membrane glycerophospholipids generated by the remodeling pathway in mammalian cells. J Lipid Res 55(5):799. https://doi.org/10.1194/jlr.R046094
14. Hishikawa D, Valentine WJ, Hishikawa YL, Shindou H, Shimizu T (2017) Metabolism and functions of docosahexaenoic acid-containing membrane glycerophospholipids. FEBS Lett 591:2730–2744. https://doi.org/10.1002/1873-3468.12825
15. Jeleń H, Błaszczyk L, Chełkowski J et al (2013) Formation of 6-*n*-pentyl-2*H*-pyran-2-one (6-PAP) and other volatiles by different *Trichoderma* species. Mycol Prog 13(3):589–600. https://doi.org/10.1007/s11557-013-0942-2
16. Kabelitz N, Santos PM, Heipieper HJ (2003) Effect of aliphatic alcohols on growth and degree of saturation of membrane lipids in *Acinetobacter calcoaceticus*. FEMS Microbiol Lett 220:223–227. https://doi.org/10.1016/s0378-1097(03)00103-4
17. Kilpinen L, Sahle FT, Oja S et al (2013) Aging bone marrow mesenchymal stromal cells have altered membrane glycerophospholipid composition and functionality. J Lipid Res 54:622–635. https://doi.org/10.1194/jlr.M030650
18. Lattif AA, Mukherjee PK, Chandra J, Roth MR, Welti R, Rouabhia M, Ghannoum MA (2011) Lipidomics of *Candida albicans* biofilms reveals phase-dependent production of phospholipid molecular classes and role for lipid rafts in biofilm formation. Microbiology 157:3232–3242. https://doi.org/10.1099/mic.0.051086-0
19. Meer GV, Voelker DR, Feigenson GW (2008) Membrane lipids: where they are and how they behave. Nat Rev Mol Cell Biol 9:112–124. https://doi.org/10.1038/nrm2330
20. Monte E (2001) Understanding *Trichoderma*: between biotechnology and microbial ecology. Int Microbiol 4:1–4. https://doi.org/10.1007/s101230100001
21. Mukherjee PK, Horwitz BA, Kenerley CM (2012) Secondary metabolism in *Trichoderma*—a genomic perspective. MBio 158:35–45. https://doi.org/10.1099/mic.0.053629-0
22. Nielsen KF, Fenhan TG, Zafari D et al (2005) Trichothecene Production by *Trichoderma brevicompactum*. J Agric Food Chem 53(21):8190. https://doi.org/10.1021/jf051279b
23. Oda S, Isshiki K, Ohashi S (2009) Production of 6-pentyl-α-pyrone with *Trichoderma atroviride* and its mutant in a novel extractive liquid-surface immobilization (Ext-LSI) system. Process Biochem 44:625–630. https://doi.org/10.1016/j.procbio.2009.01.017
24. Rainville PD, Stumpf CL, Shockcor JP et al (2007) Novel application of reversed-phase UPLC-oaTOF-MS for lipid analysis in complex biological mixtures: a new tool for lipidomics. J Proteome Res 6(2):552–558. https://doi.org/10.1021/pr060611b
25. Rawicz W, Olbrich KC, McIntosh T et al (2000) Effect of chain length and unsaturation on elasticity of lipid bilayers. Biophys J 79(1):328–339. https://doi.org/10.1016/s0006-3495(00)76295-3
26. Szule JA, Fuller NL, Rand RP (2002) The effects of acyl chain length and saturation of diacylglycerols and phosphatidylcholines on membrane monolayer curvature. Biophys J 83(2):977–984. https://doi.org/10.1016/s0006-3495(02)75223-5
27. Tarus PK, Lang'Atthoruwa CC, Wanyonyi AW et al (2003) Bioactive metabolites from *Trichoderma harzianum* and *Trichoderma longibrachiatum*. Bull Chem Soc Ethiop 17(2):185–190
28. Tijerino A, Hermosa R, Cardoza RE et al (2011) Overexpression of the *Trichoderma brevicompactum* tri5 gene: effect on the expression of the trichodermin biosynthetic genes and on tomato seedlings. Toxins (Basel) 3:1220–1232. https://doi.org/10.3390/toxins3091220
29. Turk M, Mejanelle L, Sentjurc M, Grimalt JO, Cimerman GN, Plemenitas A (2004) Salt-induced changes in lipid composition and membrane fluidity of halophilic yeast-like melanized

fungi. Extremophiles 8:53–61. https://doi.org/10.1007/s00792-003-0360-5
30. Van MG (2005) Cellular lipidomics. EMBO J 24(18):3159. https://doi.org/10.1038/sj.emboj.7600798
31. Verma M, Sk Brar, Tyagi RD et al (2007) Antagonistic fungi, *Trichoderma* spp.: panoply of biological control. Biochem Eng J 37:1–20. https://doi.org/10.1016/j.bej.2007.05.012
32. Welti R, Li W, Li M et al (2002) Profiling membrane lipids in plant stress responses. Role of phospholipase D alpha in freezing-induced lipid changes in *Arabidopsis*. J Biol Chem 277:31994–32002. https://doi.org/10.1074/jbc.M205375200
33. Wenk MR (2010) Lipidomics: new tools and applications. Cell 143:888–895. https://doi.org/10.1016/j.cell.2010.11.033
34. Xia J, Jones AD, Lau MW et al (2011) Comparative lipidomic profiling of xylose-metabolizing *S. cerevisiae* and its parental strain in different media reveals correlations between membrane lipids and fermentation capacity. Biotechnol Bioeng 108:12–21. https://doi.org/10.1002/bit.22910
35. Xu P, Shen T, Liu WP et al (2013) The elicitation effect of pathogenic fungi on trichodermin production by Trichoderma brevicompactum. Sci World J. https://doi.org/10.1155/2013/607102
36. Xu P, Shen T, Zhan XH et al (2014) Antifungal activity of metabolites of the endophytic fungus *Trichoderma brevicompactum* from garlic. Braz J Microbiol 45(1):248. https://doi.org/10.1590/s1517-83822014005000036
37. Yan X, Chen D, Xu J et al (2011) Profiles of photosynthetic glycerolipids in three strains of Skeletonema, determined by UPLC-Q-TOF-MS. J Appl Phycol 23(2):271–282. https://doi.org/10.1007/s10811-010-9553-3
38. Yin GL, Wang WM, Sha S et al (2010) Inhibition and control effects of the ethyl acetate extract of *Trichoderma harzianum* fermented broth against *Botrytis cinerea*. Afr J Microbiol Res 4(15):1647–1653